Colloidal Silica Templating Synthesis of Carbonaceous Monoliths Assuring Formation of Uniform Spherical Mesopores and Incorporation of Inorganic Nanoparticles†

Mietek Jaroniec,*,‡ Jerzy Choma,§ Joanna Gorka,‡ and Aleksandra Zawislak§

Department of Chemistry, Kent State University, Kent, Ohio 44242, and Institute of Chemistry, Military Technical Academy, 00-908 Warsaw, Poland

Received July 27, 2007. Revised Manuscript Received October 8, 2007

Colloidal silica templating synthesis was successfully used to prepare carbon monoliths with uniform spherical pores. Uniformity of the mesopores was assured by formation of a phenolic resin-type carbon precursor on the entire surface of a monolithic colloidal silica template pretreated with oxalic acid as a catalyst. Carbonization of the phenolic resin present in the pores of the colloidal silica template followed by silica dissolution afforded monolithic carbons with tailorable pore sizes reflecting the sizes of the silica colloids used. This synthesis strategy is also convenient for the introduction of metal and metal oxide nanoparticles into mesoporous carbon monoliths. Additional activation of the aforementioned carbon monoliths with KOH introduced substantial microporosity, which makes these materials attractive for a variety of applications, including adsorption and catalysis.

Introduction

One of the major advances in the area of ordered mesoporous materials, initiated in 1992 by the pioneering work on self-assembly synthesis of ordered mesoporous silicas (OMSs),[1] was a successful application of OMSs as hard templates for the synthesis of ordered mesoporous carbons (OMCs).[2–4] Although the hard-templating synthesis of OMCs is more laborious than the recently reported soft-templating approach,[5–8] it remains a very popular method for the synthesis of novel carbon nanostructures (see recent review articles[9–13] and references therein). The hard-templating (nanocasting) route includes fabrication of a silica-based template, infiltration of the template pores with carbon precursors, carbonization of the precursors, and template dissolution. Although there are numerous OMSs available as potential hard templates, their use in the OMC synthesis is somewhat limited because of inherent limitations in tailoring the pore walls in OMSs. The pore walls of most OMSs can vary over only a narrow range (1−5 nm). Since inverse replication of OMS templates transforms their pore walls into pores, pore-width tailoring in OMS-templated OMCs is limited to a rather narrow range of sizes as well.

The use of colloidal silica and colloidal silica crystals (CSCs) instead of OMSs as hard templates eliminates the aforementioned limitation because silica colloids with tailored diameters exceeding ∼5 nm can be prepared relatively easily. Also, a variety of colloidal silica solutions are available commercially. Therefore, use of colloidal silica templates for the synthesis of mesoporous carbons has generated great interest, which to some extent has been initiated by two landmark works, one devoted to ordered macroporous carbons[14] and the other to large-pore polymers.[15] Initially, polymerization of resorcinol and formaldehyde (carbon precursors) was performed in the presence of an aqueous sol of silica colloids (the pore-forming agent) to create a silica-polymer composite, which after carbonization and silica dissolution afforded mesoporous carbon.[16] In order to prevent agglomeration of the silica colloids, they were stabilized with surfactants prior to their addition to the synthesis mixture.[17] Although the synthesis strategy involving polymerization of carbon precursors in the presence of a colloidal silica sol is simple, it presents a major challenge: how to achieve the formation of uniform spherical mesopores that reflect the

† Part of the "Templated Materials Special Issue".

* Corresponding author. E-mail: jaroniec@kent.edu.
‡ Kent State University.
§ Military Technical Academy.

(1) Kresge, C. T.; Leonowicz, M. E.; Roth, W. J.; Vartuli, J. C.; Beck, J. S. *Nature* **1992**, *359*, 710–712. Beck, J. S.; Vartuli, J. C.; Roth, W. J.; Leonowicz, M. E.; Kresge, C. T.; Schmitt, K. D.; Chu, C. T.-W.; Olson, D. H.; Sheppard, E. W.; McCullen, S. B.; Higgins, J. B.; Schlenker, J. L. *J. Am. Chem. Soc.* **1992**, *114*, 10834–10843.
(2) Ryoo, R.; Joo, S. H.; Jun, S. *J. Phys. Chem. B* **1999**, *103*, 7743–7746.
(3) Lee, J.; Yoon, S.; Hyeon, T.; Oh, S. M.; Kim, K. B. *Chem. Commun.* **1999**, 2177–2178.
(4) Jun, S.; Joo, S. H.; Ryoo, R.; Kruk, M.; Jaroniec, M.; Liu, Z.; Ohsuna, T.; Terasaki, O. *J. Am. Chem. Soc.* **2000**, *122*, 10712–10713.
(5) Liang, C.; Hong, K. L.; Guiochon, G. A.; Mays, J. W.; Dai, S. *Angew. Chem., Int. Ed.* **2004**, *43*, 5785–5789.
(6) Zhang, F. Q.; Meng, Y.; Gu, D.; Yan, Y.; Yu, C. Z.; Tu, B.; Zhao, D. Y. *J. Am. Chem. Soc.* **2005**, *127*, 13508–13509.
(7) Liang, C.; Dai, S. *J. Am. Chem. Soc.* **2006**, *128*, 5316–5317.
(8) Meng, Y.; Gu, D.; Zhang, F.; Shi, Y.; Cheng, L.; Feng, D.; Wu, Z.; Chen, Z.; Wan, Y.; Stein, A.; Zhao, D. *Chem. Mater.* **2006**, *18*, 4447–4465.
(9) Ryoo, R.; Joo, S. H.; Kruk, M.; Jaroniec, M. *Adv. Mater.* **2001**, *13*, 667–680.
(10) Lee, J.; Han, S.; Hyeon, T. *J. Mater. Chem.* **2004**, *14*, 478–486.
(11) Yang, H. F.; Zhao, D. Y. *J. Mater. Chem.* **2005**, *15*, 1217–1231.
(12) Lu, A. H.; Schuth, F. *Adv. Mater.* **2006**, *18*, 1793–1805.
(13) Lee, J.; Kim, J.; Hyeon, T. *Adv. Mater.* **2006**, *18*, 2073–2094.
(14) Zakhidov, A. A.; Baughaman, R. H.; Iqbal, Z.; Cui, C.; Khayrullin, I.; Dantas, S. O.; Marti, J.; Ralchenko, V. G. *Science* **1998**, *282*, 897–901.
(15) Johnson, S. A.; Ollivier, P. J.; Mallouk, T. E. *Science* **1999**, *283*, 963–965.
(16) Han, S.; Hyeon, T. *Carbon* **1999**, *37*, 1645–1647.
(17) Han, S.; Hyeon, T. *Chem. Commun.* **1999**, 1955–1956.

10.1021/cm7020643 CCC: $40.75
Published on Web 11/20/2007

size of the colloids used. Frequently, a broad pore-size distribution (PSD) has been obtained because larger colloidal agglomerates were templated instead of single colloids.[16–18]

Formation of colloid-templated carbons with uniform spherical mesopores requires that the entire surface of the colloidal silica template be fully covered with carbon precursors. This requirement can be achieved by controlling the interpenetration of mesophase pitch particles and silica colloids with the help of suitable heating, stabilization, and carbonization,[19–21] by completely filling the pores of the colloidal silica templates to form the true inverse carbon replicas,[18,22] and by film-type replication of the aforementioned templates.[23,24] Complete filling of the pores in the CSC template affords carbons with tailorable spherical mesopores, but their pore volumes cannot exceed 1.36 cm^3/g.[24] However, formation of a thin carbon film on the entire surface of the colloidal silica template, achieved by surface-catalyzed polymerization of resorcinol and crotonaldehyde, afforded large-pore-volume (LPV) carbons with total volumes reaching 9 cm^3/g.[23,24]

Another important topic in the area of mesoporous carbons is the fabrication of carbon monoliths. So far, silica monoliths with disordered nonuniform mesopores (such as those prepared using the sol–gel method reported by Nakanishi et al.[25]) have mainly been used to fabricate the corresponding carbon monoliths.[26–30] Another method for the fabrication of carbon monoliths involves mixing porous silica particles (such as SBA-15 or zeolites) with sucrose, followed by carbonization and silica dissolution.[31–34] This method was significantly extended by Lu et al.,[32] who used NaCl and SBA-15 particles to create a hierarchical porous structure in carbon monoliths. In this case, poly(furfuryl alcohol) was used as the carbon precursor instead of sucrose. This method is a modification of nanocasting strategy, in which an excess of carbon precursor is used as a binder of SBA-15 particles; the carbon monolith is obtained by carbonization and silica dissolution of the aforementioned composite.

In this work we have applied colloidal templating (which allows one to tailor the pore size in the resulting carbons by varying the size of silica colloids and to achieve a large pore volume by employing film-type replication) to the inverse replication of colloidal silica monoliths. The colloidal templating synthesis afforded mesoporous carbon monoliths with tailorable uniform spherical mesopores and large pore volume. This synthesis strategy is particularly valuable for the incorporation of inorganic nanoparticles into carbon monoliths, which we tested through the preparation of a silver-containing carbon. Also, KOH activation was used to obtain microporous−mesoporous carbons with high surface areas and large micropore volumes. Further developments are possible in this area, such as employing core-shell nanoparticles for the fabrication of monolithic templates and carbons with embedded inorganic nanoparticles.

Experimental Section

(1) Synthesis of Carbon Monoliths with Uniform Spherical Mesopores. Mesoporous carbon (MC) monoliths were prepared using colloidal silica templates in the monolithic form. The latter were prepared by drying a commercially available aqueous suspension of silica colloids containing 40 wt % silica and having an average colloid size of 24 nm (Ludox AS-40, Sigma-Aldrich Chemie), filling cylindrical steel vessels (1.3 cm in diameter and 1.5 cm in height) with the silica powder, and compressing this powder under a pressure of 3 MPa. Next, the resulting mesoporous silica (MS) monoliths were sintered by heating to 700 °C at a heating rate of 1 °C/min and then maintaining this temperature for 0.5 h.

The MC monoliths were synthesized as in our previous work.[23,24] One gram of the MS template was impregnated with 40 mg of anhydrous 97% oxalic acid (Fluka), which was used as a catalyst. This impregnation was performed by immersing the MS monolith in an ethanol solution of oxalic acid for 10 min. The impregnated template was dried for 2 h at 90 °C in order to evaporate the ethanol. Next, the oxalic acid-treated MS monolith was impregnated with a mixture containing 2.38 g of 98% resorcinol (Sigma-Aldrich) and 2.1 cm^3 of 98% crotonaldehyde (Fluka) over 30 min. Subsequently, the resulting composite sample was subjected to a series of thermal treatments. The first treatment was carried out at 60 °C for 0.5 h. The second treatment was carried out at 120 °C for ∼10 h (during which initial prepolymerization was indicated by a color change to orange). The actual polymerization was performed at 200 °C for 5 h (the composite sample was a dark-brown color). In the final thermal treatment, the resulting sample was transferred to a tube furnace for carbonization under nitrogen at 900 °C for 2 h, using a heating rate of 2 °C/min. The silica template was removed using 15% hydrofluoric acid (Chempur). The resulting MC monolith was rinsed with butanol (Chempur), hexane (Chempur), and distilled water and dried in an oven at 80 °C for ∼12 h. The yield of the synthesis was 2 g of carbon. Duplicate MS monoliths (designated MS-1 and MS-2) were prepared and used as hard templates to prepare the corresponding MC monoliths (MC-1 and MC-2).

(2) Synthesis of Mesoporous Carbon Monoliths Containing Silver Nanoparticles. One gram of colloidal silver powder having 99.5% purity and particle sizes less than 70 nm (Sigma-Aldrich Chemie) was added to 23.2 cm^3 of Ludox AS-40. The resulting colloidal suspension of silver and silica (containing 10 wt % silver in relation to silica) was dried at 80 °C under intensive stirring. After almost-complete evaporation of the water, the drying process was continued in an oven at 75 °C for 12 h. The resulting powder

(18) Gierszal, K. P.; Yoon, S. B.; Yu, J. S.; Jaroniec, M. *J. Mater. Chem.* **2006**, *16*, 2819–2823.
(19) Li, Z.; Jaroniec, M. *J. Am. Chem. Soc.* **2001**, *123*, 9208–9209.
(20) Li, Z.; Jaroniec, M. *Chem. Mater.* **2003**, *15*, 1327–1333.
(21) Li, Z.; Jaroniec, M. *Anal. Chem.* **2004**, *76*, 5479–5485.
(22) Yoon, S. B.; Chai, G. S.; Kang, S. K.; Yu, J.-S.; Gierszal, K. P.; Jaroniec, M. *J. Am. Chem. Soc.* **2005**, *127*, 4188–4189.
(23) Gierszal, K. P.; Jaroniec, M. *J. Am. Chem. Soc.* **2006**, *128*, 10026–10027.
(24) Gierszal, K. P.; Jaroniec, M. *J. Phys. Chem. C* **2007**, *111*, 9742–9748.
(25) Nakanishi, K.; Soga, N. *J. Non-Cryst. Solids* **1992**, *139*, 1–13.
(26) Hu, Y. S.; Adelhelm, P.; Smarsly, B. M.; Hore, S.; Antonietti, M.; Maier, J. *Adv. Funct. Mater.* **2007**, *17*, 1873–1878.
(27) Shi, Z. G.; Feng, Y. Q.; Xu, L.; Da, S. L.; Zhang, M. *Carbon* **2003**, *41*, 2653–2689.
(28) Shi, Z. G.; Feng, Y. Q.; Xu, L.; Da, S. L.; Liu, Y. *Mater. Chem. Phys.* **2006**, *97*, 472–475.
(29) Wang, L.; Lin, S.; Lin, K.; Yin, C.; Liang, D.; Di, Y.; Fan, P.; Jiang, D.; Xiao, F. S. *Microporous Mesoporous Mater.* **2005**, *85*, 136–142.
(30) Wang, L.; Zhao, Y.; Lin, K.; Zhao, X.; Shan, Z.; Di, Y.; Sun, Z.; Cao, X.; Zou, Y.; Jiang, D.; Jiang, L.; Xiao, F. S. *Carbon* **2006**, *44*, 1298–1352.
(31) Klepel, O.; Srauβ, H.; Garsuch, A.; Böhme, K. *Mater. Lett.* **2007**, *61*, 2037–2039.
(32) Lu, A. H.; Li, W. C.; Schmidt, W.; Schuth, F. *Microporous Mesoporous Mater.* **2006**, *95*, 187–192.
(33) Liang, C.; Dai, S.; Guiochon, G. *Anal. Chem.* **2003**, *75*, 4904–4912.
(34) Taguchi, A.; Smatt, J. H.; Linden, M. *Adv. Mater.* **2003**, *15*, 1209–1211.

was placed in the cylindrical steel vessel (described above) and compressed under a pressure of 3 MPa to obtain the mesoporous silica monolith with silver nanoparticles. These silver-containing mesoporous silica (MS-Ag) monoliths were sintered by heating to 700 °C at a heating rate of 1 °C/min and then maintaining this temperature for 0.5 h.

The silver-containing mesoporous carbon (MC-Ag) monolith was prepared using the MS-Ag monolith as a hard template according to the procedure described above for MC monoliths.

(3) KOH Activation of Carbon Monoliths. The MC-2 monolith (1.67 g) was impregnated with KOH solution (36 g of KOH in 10 cm^3 of water) at 80 °C over 4 h. The KOH-impregnated MC-2 monolith was dried at 105 °C for 10 h. The KOH/carbon weight ratio in the dry product was 0.6. The activation process for the KOH-impregnated MC-2 monolith was carried out by heating the sample to 700 °C under flowing nitrogen in a tube furnace at a rate of 10 °C/min and then maintaining this temperature for 45 min. After the resulting monolith was cooled in flowing nitrogen, it was washed successively with 0.1 M HCl solution and deionized water to ensure that the KOH was completely removed. Finally, the activated MC-2 monolith was dried at 105 °C for 12 h, and the final microporous−mesoporous carbon monolith was denoted as MMC-2.

(4) Measurements and Characterization. Powder X-ray diffraction (XRD) measurements on the silver-containing MC monolith were conducted using an X'Pert Pro MPD multipurpose diffractometer (PANalytical, Inc.) with Cu Kα radiation (1.5406 Å) at room temperature over a wide range of angles ($10.0° < 2\theta < 80.0°$) using an operating voltage of 40 kV, a step size of 0.020°, and a step time of 3 s.

Scanning electron microscopy (SEM) images were taken using a Zeiss LEO 1530 microscope operating under a voltage of 20 kV.

Carbon samples for transmission electron microscopy (TEM) were prepared by grinding followed by ultrasonic treatment in isopropyl alcohol for 1 min. A drop of the suspension was dried on the standard TEM sample grid covered with holey carbon film. A JEOL 2000 electron microscope operating at 80 kV was used for observations.

Nitrogen adsorption isotherms were measured at −196 °C on ASAP 2010 and 2020 volumetric analyzers (Micromeritics, Inc., Norcross, GA) using gas having 99.998% purity. Before adsorption measurements each sample was outgassed under vacuum for 2 h at 200 °C.

The Brunauer–Emmett–Teller (BET) specific surface area was calculated from the nitrogen adsorption isotherm in the range of relative pressures from 0.05 to 0.20 using a cross-sectional area of 0.162 nm^2 per nitrogen molecule.[35] The single-point pore volume[36] was estimated from the volume adsorbed at a relative pressure of ~0.99. Since the pore geometry in the MS and MC monoliths is different (in the case of the MS monolith templates, each mesopore represents the space between densely packed silica spheres, whereas the mesopores of the MC monoliths are spherical), we used the Barrett–Joyner–Halenda (BJH) method[37] for an approximate estimation of pore sizes. This analysis was performed using adsorption branches of nitrogen adsorption/desorption isotherms. To improve the BJH pore-size analysis, we used the statistical film thickness curves for nitrogen on silica[38] and carbon[39] surfaces obtained from nitrogen adsorption isotherms measured on LiChrospher Si-1000 macroporous silica (Merck)[40] and BP280 carbon black (Cabot).[41] The pore width at the maximum of the BJH pore-size distribution was used for characterization of the samples studied.

In addition, α_s-plot analysis[42] was used to estimate the volume of micropores in the samples studied. This analysis was performed using the standard reduced adsorption data reported for nitrogen on the aforementioned silica and carbon reference materials.[40,41]

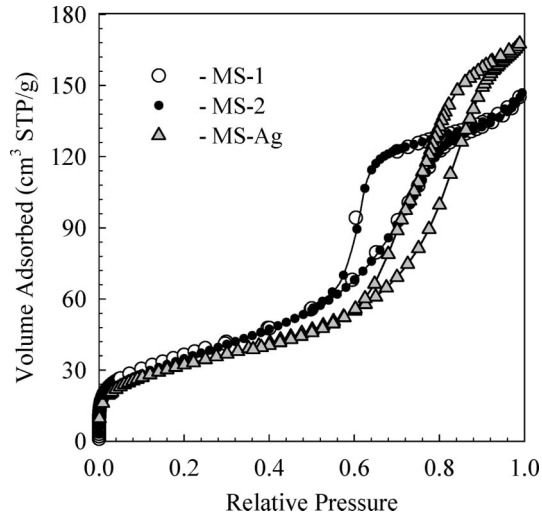

Figure 1. Nitrogen adsorption isotherms at −196 °C for the MS-1 and MS-2 templates composed of 24 nm silica colloids and the MS-Ag colloidal silica template containing silver nanoparticles.

Table 1. Adsorption Parameters for the Colloidal Silica Templates

silica template	BET surface area (m^2/g)	pore volume (cm^3/g)	pore width (nm)
MS-1	132	0.22	7
MS-2	129	0.22	7
MS-Ag	117	0.26	11

Results and Discussion

(1) Colloidal Silica Templates. Two colloidal silica templates were prepared by compressing powders obtained by drying an aqueous solution of 24 nm silica colloids. Nitrogen adsorption isotherms measured on these siliceous templates are shown in Figure 1. These are type-IV isotherms, which are characteristic of mesoporous solids. The two samples had very similar adsorption parameters (see Table 1), indicating good reproducibility of the method used to fabricate the templates from colloidal silica. The BET specific surface areas and the total pore volumes for both samples were ~130 m^2/g and 0.22 cm^3/g, respectively. This pore volume corresponds to a packing degree of 67.4%, which is smaller than the value of 74% obtained for ideal packing of monodisperse silica spheres [packing degree = 1 − porosity = 1/(1 + pore volume × density of silica)]. Thus, the method used for fabrication of the colloidal silica templates did not ensure the formation of colloidal crystals. Therefore, the resulting templates were not ordered (see the SEM images in Figure S1 of the Supporting Information); consequently, the corresponding carbon replicas were also

(35) Brunauer, S.; Emmet, P. H.; Teller, E. *J. Am. Chem. Soc.* **1938**, *60*, 309–319.
(36) Kruk, M.; Jaroniec, M. *Chem. Mater.* **2001**, *13*, 3169–3183.
(37) Barrett, E. P.; Joyner, L. G.; Halenda, P. P. *J. Am. Chem. Soc.* **1951**, *73*, 373–380.
(38) Kruk, M.; Jaroniec, M.; Sayari, A. *Langmuir* **1997**, *13*, 6267–6273.
(39) Choma, J.; Jaroniec, M.; Kloske, M. *Adsorpt. Sci. Technol.* **2002**, *20*, 307–315.
(40) Jaroniec, M.; Kruk, M.; Olivier, J. *Langmuir* **1999**, *15*, 5410–5413.
(41) Kruk, M.; Jaroniec, M.; Gadkaree, K. P. *J. Colloid Interface Sci.* **1997**, *192*, 250–256.
(42) Jaroniec, M.; Kaneko, K. *Langmuir* **1997**, *13*, 6589–6596.

disordered. However, they consisted of uniform and spherical mesopores if the silica colloids used to obtain the templates were uniform and spherical. While the presence of uniform and interconnected mesopores is beneficial for many applications, at the present time no significant advantages of ordered porosity are known.

The estimated values of the BJH pore width at the PSD maximum (see Figure S2 in the Supporting Information) were 7 nm for both the MS-1 and MS-2 templates. These values are approximate because the BJH method[37] applies for cylindrical pores, whereas the pores in colloidal silica templates represent nanospaces between adjacent spherical silica colloids. Since no pore-size analysis method exists for this pore geometry, the BJH method was used. However, the aforementioned pore size is realistic because it is comparable to the size of mesopores present in ideal colloidal crystals consisting of 24 nm silica particles.

Figure 1 also shows the nitrogen adsorption isotherm for the MS-Ag template, which was fabricated from 24 nm silica colloids with addition of 10 wt % silver nanoparticles. Since the silver nanoparticles were larger than the silica colloids, the resulting silver−silica template had a larger pore volume and a larger average pore width than those for the purely siliceous templates (Table 1), indicating a smaller packing density. Also, introduction of the larger silver nanoparticles into the colloidal silica template increased the nonuniformity of the resulting porous system, as indicated by the decreased steepness of the capillary condensation step on the MS-Ag adsorption isotherm in comparison with those observed for the MS-1 and MS-2 templates (Figure 1).

(2) Mesoporous Carbon Monoliths. The MS-1 and MS-2 templates (Table 1) composed of 24 nm silica colloids were used to prepare the monolithic carbons as shown in the left column of Scheme 1. This scheme illustrates the process of fabricating a monolithic carbon replica by completely filling the mesopores in the silica template with the carbon matrix. In addition, Scheme 2 illustrates film-type replication, which is carried out by forming a thin carbonaceous film on the walls of the template mesopores; in this case, the interior of mesopores is not filled, which creates extra porosity in the resulting carbon.[23]

The carbon monoliths (see the pictures of actual monoliths in Scheme 1) were fabricated using the same recipe as that employed for the synthesis of LPV carbons by film-type replication of powdered colloidal silica templates (Scheme 2).[23,24] One of the important steps in this replication method is coating the entire surface of the siliceous template with the oxalic acid catalyst; this procedure assures polymerization of resorcinol and crotonaldehyde in the form of a thin film that fully covers the entire surface of the template. Carbonization of this polymeric film and template dissolution affords the LPV carbons. As shown elsewhere,[23,24] this approach was successful for the synthesis of the LPV carbons when powdered colloidal silica templates were used. Here we have demonstrated that oxalic acid coating and resorcinol−crotonaldehyde polymerization can also be performed effectively in the pores of colloidal silica monoliths, making possible the preparation of mesoporous carbon monoliths (see the left column of Scheme 1). The specific surface area can be significantly increased by creation of microporosity in these carbon monoliths through activation (the last step in Scheme 1).

Scheme 1. Illustration of the Fabrication of Mesoporous Carbons (Left Column) and Mesoporous Carbons with Incorporated Inorganic (e.g., Silver) Nanoparticles (Right Column), Including Pictures of Actual Monoliths at Different Stages of the Fabrication Process (Middle Column)[a]

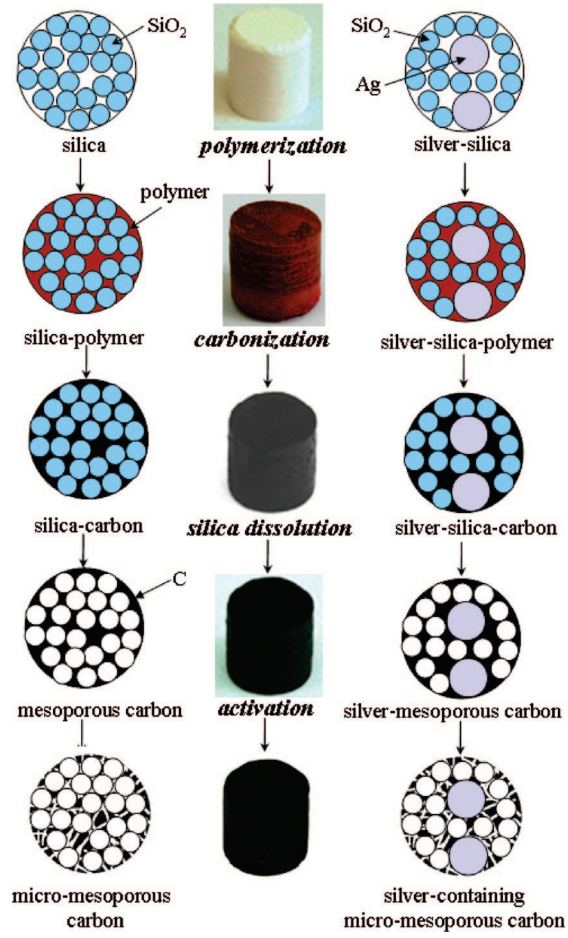

[a] Identification of monoliths: hard template fabricated by compressing powdered colloidal silica (white), silica−polymer nanocomposite prepared by polymerization of resorcinol and crotonaldehyde in the pores of the colloidal silica template (brown), silica−carbon nanocomposite obtained by carbonization of the polymer in the aforementioned silica−polymer composite (dark gray), mesoporous carbon obtained by removal (dissolution) of silica from the silica−carbon composite (black), and micro−mesoporous carbon obtained by KOH activation of the colloid-templated mesoporous carbon (black).

A major advantage of the method used here for the fabrication of colloidal silica monoliths is the possibility of introducing various inorganic nanoparticles, such as metals and metal oxides, into the siliceous template. These nanoparticles can be introduced simply by adding them into the colloidal solution, as described in the Experimental Section. If the nanoparticles withstand the process of removing the silica template, the current recipe affords carbon monoliths containing the nanoparticles, which are accessible through the interconnected spherical mesopores created during dissolution of the silica colloids, as illustrated in the right

Scheme 2. Illustration of Film-Type Replication of Colloidal Silica Templates

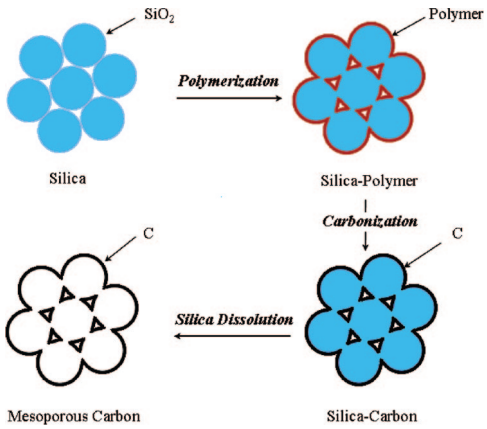

column of Scheme 1 for silver nanoparticles. This procedure represents a simple and feasible way to introduce many inorganic nanoparticles of different sizes and shapes into mesoporous carbon monoliths as well as to control their loading.

Figure 2 shows nitrogen adsorption isotherms for the two MC monoliths MC-1 and MC-2 and the silver-containing monolith MC-Ag, which were fabricated using the MS-1, MS-2, and MS-Ag templates listed in Table 1, respectively. These are type-IV isotherms with steep capillary condensation steps and H1-type hysteresis loops, which are characteristic of uniform and fully accessible mesopores. Values of the adsorption parameters evaluated from these isotherms (BET surface area, pore volume, and pore size) are summarized in Table 2. As this table shows, the pore sizes of all the carbon monoliths studied are very similar, which is expected because these monoliths were all prepared from silica colloids of the same size. The pore size corresponding to the condensation pressure indicated by the steep condensation step is 27 nm (Table 2), whereas the size of the pore openings estimated from the steep desorption branch is about 10 nm. The corresponding pore-size distributions (Figure S3 in the Supporting Information) all show a main peak near 27 nm (pores after dissolution of silica colloids), a small

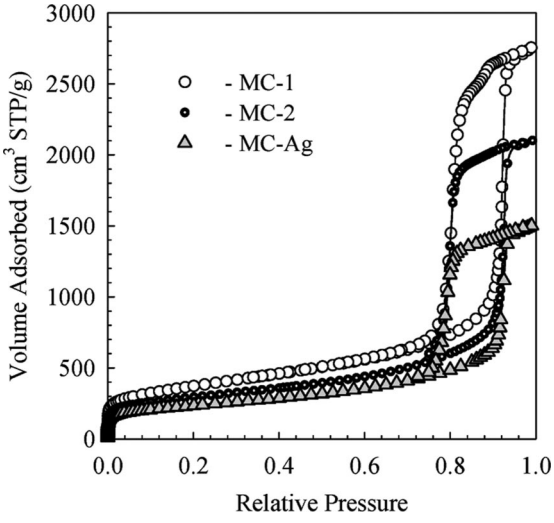

Figure 2. Nitrogen adsorption isotherms at −196 °C for the mesoporous carbon monoliths without (MC-1 and MC-2) and with silver nanoparticles (MC-Ag).

Table 2. Adsorption Parameters for the Mesoporous Carbon Monoliths[a]

carbon monolith	BET surface area (m^2/g)	pore volume (cm^3/g)	micropore volume (cm^3/g)	pore width (nm)
MC-1	1300	4.26	0.19	26.8
MC-2	1040	3.25	0.14	27.6
MC-Ag	830	2.32	0.10	27.0
MMC-2	2340	2.58	0.77	28.7

[a] Column 3 gives values of the single-point pore volume corresponding to a relative pressure of ~0.99; the micropore volume was evaluated by α_s-plot analysis.

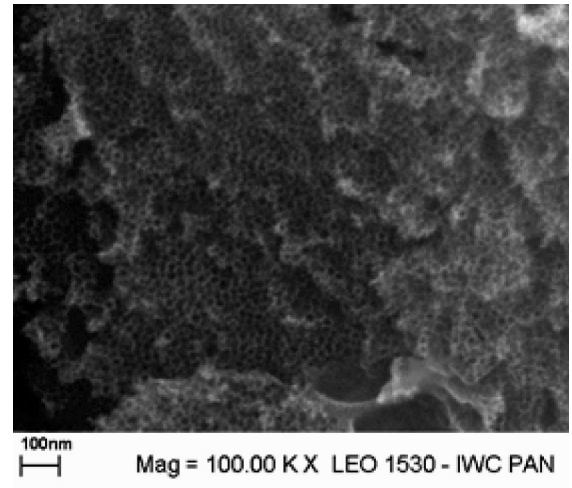

Figure 3. SEM image of the mesoporous carbon monolith MC-1.

peak near 5 nm (pores formed as a result of failure to completely fill template mesopores with the carbon precursors), and an intermediate peak near 2 nm (micropores). The steep capillary condensation steps on the adsorption isotherms (Figure 2) and the consequent narrow PSDs (Figure S3 in the Supporting Information) indicate that the recipe used here produced a quite uniform coating of the pore walls of the colloidal silica monoliths with resorcinol−crotonaldehyde polymer and that this uniformity was preserved during the carbonization process. Thus, if colloidal silica with a very narrow PSD is used for the template fabrication, this recipe affords carbons with uniform spherical mesopores that are interconnected but disordered (see Figure 3). In order to obtain monolithic carbon replicas with ordered mesopores, the colloidal silica crystals should be used as hard templates.

The pore volumes of the two carbon monoliths, which were obtained by replication of the almost identical monolithic silica templates MS-1 and MS-2, were different (see Table 2). Since the pore volumes for the MC monoliths studied were quite large (4.26 and 3.25 cm^3/g), film-type replication occurred;[24] note that in the case of complete filling of template pores with carbon (which has a true density of 2.1 g/cm^3), the pore volume of the inverse nonmicroporous carbon replica should not exceed 1.36 cm^3/g.[24] The observed difference in the pore volumes of the MC-1 and MC-2 carbon monoliths indicates that precise control of experimental conditions, especially the molar composition of carbon precursors, is required in order to achieve good reproducibility of this quantity. A quantitative analysis of the theoretical relationships between the structural parameters for the silica templates and their inverse carbon replicas[24]

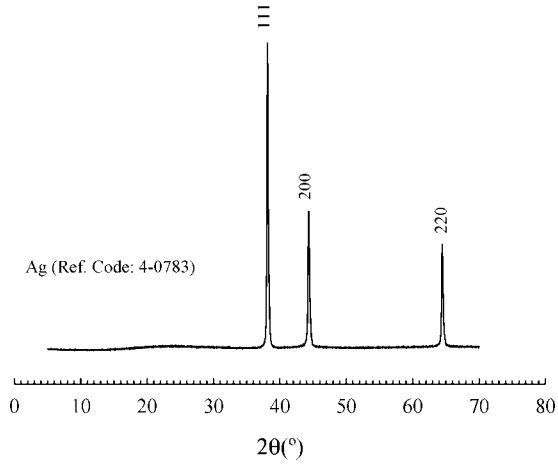

Figure 4. Wide-angle XRD pattern showing the presence of silver nanoparticles in the MC-Ag carbon monolith.

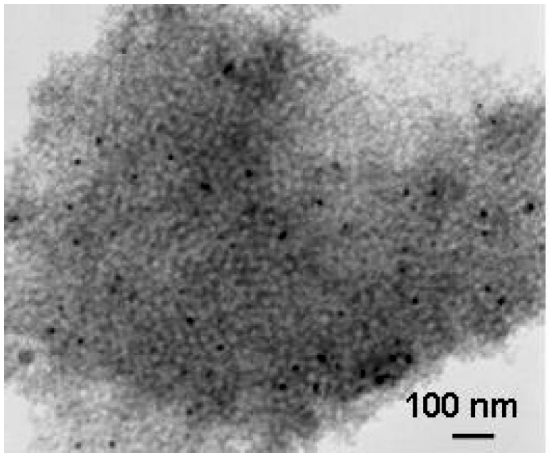

Figure 5. TEM image showing the presence of silver nanoparticles in the MC-Ag carbon monolith.

indicated that even a relatively small change in the thickness of the carbon film has a pronounced effect on the pore volume of the resulting carbon monoliths.

The nitrogen adsorption isotherm and adsorption parameters for the carbon monolith with incorporated silver nanoparticles show that the presence of silver (confirmed by the wide-angle XRD pattern in Figure 4 and the TEM images in Figure 5 and Figure S4 of the Supporting Information) did not affect the pore width (which was controlled by the size of the silica colloids used) but did affect the specific pore volume (because the nanoparticles reduced the mass of carbon per gram of the silver−carbon composite and diminished the sample volume available for the mesopores). Thermogravimetric analysis in air (see Figure S5 in the Supporting Information) gave an estimated silver content of 40.7% in the silver−carbon monolith. In order to obtain a uniform distribution of silver nanoparticles in the silver−carbon composite, the nanoparticles must be uniformly distributed in the silver−silica template. The TEM image in Figure 5 shows that the silver nanoparticles were separated in the carbon matrix, although in some images agglomerates of silver are visible (see Figure S4 in the Supporting Information). The distribution of silver nanoparticles in the carbon monoliths can be improved by reducing the silver percentage and effectively mixing the silver and silica colloids during preparation of the template.

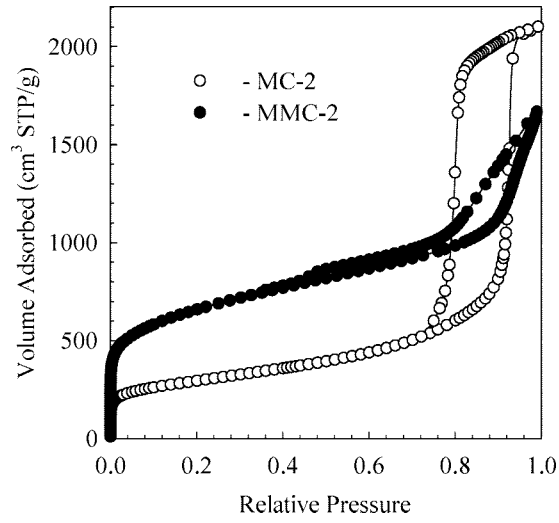

Figure 6. Comparison of nitrogen adsorption isotherms at −196 °C for the mesoporous carbon monoliths before (MC-2) and after KOH activation (MMC-2).

(3) Creation of Microporosity in Carbon Monoliths. The MC-2 carbon monolith was subjected to KOH activation as described in the Experimental Section. KOH activation has often been used to prepare carbons having high surface areas. The activation process involves various reactions on the carbon surface that are initiated by KOH decomposition and result in the formation of gaseous products (activators), mainly water and carbon dioxide; consequently, new pores are developed and existing ones may be enlarged.[43–46] KOH has been used to prepare high-surface-area carbons by direct activation of phenolic resins.[47,48] In this work, KOH activation was used to develop additional porosity in the phenolic resin-type carbon monolith MC-2, forming the microporous−mesoporous carbon monolith, MMC-2.

A comparison of the nitrogen adsorption isotherms for the MC-2 and MMC-2 carbon monoliths (Figure 6) shows that KOH activation increased the BET specific surface area by a factor of 2 and the micropore volume by a factor of 5.5 (see Table 2). The BET surface area of MMC-2 was as high as 2340 m^2/g, and the MMC-2 micropore volume obtained from α_s-plot analysis (Figure S6 in the Supporting Information), 0.77 cm^3/g, was large compared to that for MC-2 (0.14 cm^3/g). Thus, KOH activation of the MC-2 monolith increased the fraction of micropores from 4.3% to 30%. For the sample studied, the total pore volume and the volume of mesopores were reduced by the KOH activation process. This reduction was accompanied by a significant broadening of the PSD, as illustrated in Figure S7 of the Supporting Information. Since the film-type carbon replicas have relatively thin mesopore walls,[23,24] KOH activation leads not

(43) Lillo-Rodenas, M. A.; Juan-Juan, J.; Cazorla-Amoros, D.; Linares-Solano, A. *Carbon* **2004**, *42*, 1371–1375.
(44) Chunlan, L.; Shaoping, X.; Yixiong, G.; Shuqin, L.; Changhou, L. *Carbon* **2005**, *43*, 2295–2301.
(45) Park, S. J.; Jung, W. Y. *J. Colloid Interface Sci.* **2002**, *250*, 196–200.
(46) Matos, J.; Labady, M.; Albornoz, A.; Laine, J.; Brito, J. L. *J. Mol. Catal. A* **2005**, *228*, 189–194.
(47) Teng, H.; Wang, S. C. *Carbon* **2000**, *38*, 817–824.
(48) Teng, H.; Wang, S. C. *Ind. Eng. Chem. Res.* **2000**, *39*, 673–678.

only to the creation of micropores but also to the enlargement of the existing pores, causing the PSD broadening. Although monolithic morphology was preserved during activation, the mechanical stability of the activated carbon monolith was lessened significantly compared with that of the carbon monoliths before KOH activation. Further work on optimizing the KOH activation process in order to maximize the formation of micropores while simultaneously eliminating, or at least reducing, the deterioration of the mesoporous structure is in progress.

Concluding Remarks

This work has shown that the recently proposed recipe for film-type replication of colloidal silica powders is also applicable to replication of colloidal silica monoliths. The latter can be simply fabricated by compressing colloidal silica powder without or with inorganic nanoparticles. It was shown that this fabrication process is especially convenient for incorporation of various inorganic nanoparticles into the monolithic silica templates, the replication of which leads to the mesoporous carbon monoliths containing inorganic nanoparticles. The feasibility of this recipe was illustrated by the synthesis of mesoporous carbon monoliths containing silver nanoparticles. While the carbon monoliths, which were prepared by oxalic acid-catalyzed polymerization of resorcinol and crotonaldehyde in the pores of the monolithic silica templates followed by carbonization of the resulting polymer and silica dissolution, are mainly mesoporous, it was possible to significantly increase their surface areas by postsynthetic KOH activation, which created substantial microporosity.

A major advantage of the carbon monoliths studied is the presence of uniform spherical mesopores created by silica dissolution. The size of these pores can be easily tuned over a very wide range of mesopores and macropores by adjusting the size of silica colloids.[14,19–24,57] The proposed film-type inverse replication of monolithic silica-based templates permits one not only to tune the pore size but also to control the loading of nanoparticles and tailor the pore volume of the resulting carbon monoliths. This synthesis strategy is also convenient for the incorporation of nanoparticles having desired catalytic activities, magnetic properties, and so on.

One may envision the formation of monolithic templates from core–shell nanoparticles having an inorganic core (e.g., gold) and a silica shell (see Scheme 3). The synthesis of this type of core–shell nanoparticle has already been reported elsewhere.[49–56] The resulting monolithic templates could be used to create rattle-type mesoporous carbon monoliths with desired inorganic nanoparticles trapped in spherical mesopores formed by dissolution of siliceous shells. This example illustrates that the design of novel monolithic carbon mesostructures is possible, especially those with incorporated inorganic nanoparticles having desired properties.

Scheme 3. Illustration of the Fabrication of Rattle-like Carbon Monoliths Containing Inorganic (e.g., Gold) Nanoparticles[a]

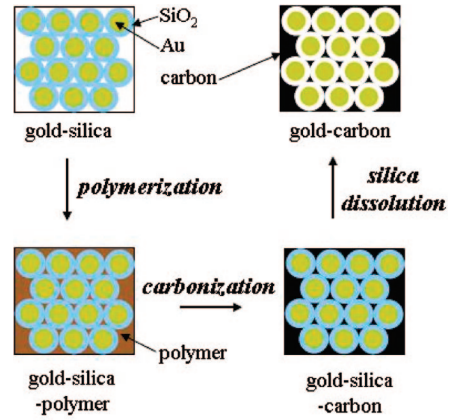

[a] This scheme illustrates the use of gold-core−silica-shell nanoparticles for the fabrication of a hard template and the corresponding mesoporous carbon replica having gold nanoparticles contained in spherical mesopores created by dissolution of the silica shells.

Acknowledgment. This research was supported in part through a subcontract to M.J. and J.G. under NIRT Grant DMR-0304508 awarded to Carnegie Mellon University from the National Science Foundation and in part by the Ministry of Science and Higher Education (Poland) under Grants 942 and 0T00C 01030 awarded to the Military Technical Academy in Warsaw. We thank Dr. Izabela Nowak from A. Mickiewicz University in Poland for TEM imaging of the silver−carbon composite.

Supporting Information Available: Figures showing SEM images for the MS-2 colloidal silica monolith, pore-size distributions for the mesoporous silica and carbon monoliths, TEM images and a thermogravimetric analysis profile for the silver−carbon monolith, and α_s-plots for a carbon monolith before and after KOH activation (PDF). This material is available free of charge via the Internet at http://pubs.acs.org.

CM7020643

(49) Tunc, I.; Demirok, U. K.; Suzer, S.; Correa-Duatre, M. A.; Liz-Marzan, L. M. *J. Phys. Chem. B* **2005**, *109*, 24182–24184.
(50) Dick, K.; Dhanasekaran, T.; Zhang, Z.; Meisel, D. *J. Am. Chem. Soc.* **2002**, *124*, 2312–2317.
(51) Botella, P.; Corma, A.; Navarro, M. T. *Chem. Mater.* **2007**, *19*, 1979–1983.
(52) Xia, X.; Liu, Y.; Backman, V.; Ameer, G. A. *Nanotechnology* **2006**, *17*, 5435–5440.
(53) Chou, K. S.; Chen, C. C. *Microporous Mesoporous Mater.* **2007**, *98*, 208–213.
(54) Zhao, W.; Gu, J.; Zhang, L.; Chen, H.; Shi, J. *J. Am. Chem. Soc.* **2005**, *127*, 8916–8917.
(55) Kobayashi, Y.; Horie, M.; Konno, M.; Rodriguez-Gonzalez, B.; Liz-Marzan, L. M. *J. Phys. Chem. B* **2003**, *107*, 7420–7425.
(56) Tartaj, P.; Serna, C. *J. Am. Chem. Soc.* **2003**, *125*, 15754–15755.
(57) Gierszal, K. P.; Jaroniec, M.; Liang, C.; Dai, S. *Carbon* **2007**, *45*, 2171–2177.